Hyperspectral Unmixing via Semantic Spectral Representations

Yuki Itoh, Siwei Feng, Marco F. Duarte, and Mario Parente
Department of Electrical and Computer Engineering
University of Massachusetts, Amherst, MA 01003, U.S.A.
Email: {yitoh,sfeng,mduarte,mparente}@umass.edu

Abstract—We propose a new spectral unmixing method using a semantic spectral representation, which is produced via non-homogeneous hidden Markov chain (NHMC) models applied to wavelet transforms of the spectra. Previous studies have shown that the representation is robust to spectral variability in the same materials because it can automatically detect the diagnostic spectral features in the training data. Therefore, our method can successfully detect materials while automatically extracting diagnostic features, showing high resilience to spectral variability.

Simulations indicate that our unmixing method could be effectively used on Hapke mixtures.

I. INTRODUCTION

Spectral unmixing aims at estimating the fractional abundances of pure spectral signatures (also called as endmembers) in each mixed pixel collected by an imaging spectrometer. Both linear [1] and nonlinear approaches [2] to unmixing have been proposed. In many situations, the identification of the endmember signatures in the original data set may be challenging due to insufficient spatial resolution, mixtures happening at different scales, and unavailability of completely pure spectral signatures in the scene.

However, the unmixing problem can also be approached by assuming that the observed image spectra can be expressed in the form of combinations of a number of pure spectral signatures known in advance (e.g., spectra collected on the ground by a field spectroradiometer or in the laboratory from field samples). Unmixing then amounts to finding the optimal subset of signatures in a (potentially very large) spectral library that can best model each mixed pixel in the scene. In particular, approaches based on sparse regression have received attention in the literature [3–5].

At their core, hyperspectral unmixing methods based on sparsity assume a linear mixing model. However, several aspects of the physical measurement introduce nonlinearities in the mixing process. While detailed nonlinear mixing models have been proposed for specific scenarios (e.g the ones introduced by Hapke that describes the scattering behavior of intimate particulate mixtures Hapke [6]), in many practical scenarios, it is difficult to assess the specific nonlinear parametric shape of mixed hyperspectral data clouds and a method for detecting endmembers that does not rely on a particular mixing model would be desirable.

Mixed spectra retain most of the diagnostic spectral information present in the endmember spectra, and this information can be leveraged in unmixing by identifying the endmember only through a set of diagnostic features. Diagnostic features are routinely manually defined by practitioners to discriminate spectral families (e.g. the Tetracorder algorithm [7]). It would be desirable to automate the process of extraction of diagnostic representations of the endmembers directly from the data.

It has been recently shown that training data in the form of material spectra can be used to automatically identify relevant diagnostic features [8, 9]. Specifically, a non-homogeneous hidden Markov chain (NHMC) model can be applied to the wavelet-domain representation of hyperspectral signatures, which automatically detects diagnostic features of each spectra in the training data set while suppressing uninformative information. Therefore, the NHMC representation enables us to identify materials independently of the mixtures observed, while automatically detecting a set of characteristic features of each material in the mixtures.

In this paper, we develop a new unmixing method using spectral representations obtained from the NHMC model. The model provides binary labels marking significant portions of the spectrum, some of which are shown to be preserved by the mixture process. We design an unmixing algorithm that searches for such discriminating labels, and is constituted by a set of endmember detectors. The algorithm makes therefore no assumptions on the mixing model that generated the data.

II. NHMC-BASED SPECTRAL UNMIXING

Assuming that we have a large spectral library, we consider the problem of detecting materials (endmembers) that are present in each observed mixture from its spectral signature. In our method, one detector is designed for each endmember, making the method independent from the pre-defined number of endmembers undergoing testing.

Our method is composed of three steps, described below, with the last two steps being illustrated in Fig. 1.

A. NHMC Model Labeling

We begin by training NHMC models using Daubechies-1 wavelet representations of a training set of mixture spectra [8–10]. Using the learned NHMC model, we obtain binary labels [8–10] for a set of pure and attenuated spectra of the endmembers. Each binary label matrix has size $S \times N$, where S is the number of wavelet scales and N is the length of the spectrum, and marks significant portions of the spectrum using "large" labels (illustrated in red) for the wavelet coefficients at the corresponding bands and scales, while assigning "small" labels (illustrated in blue) to wavelet coefficients that correspond to non-informative regions of the spectrum.

B. Learning Endmember Features

In the second stage, we identify dominant features that persist in the NHMC binary labels for an endmember even as it is attenuated. For that purpose, we build a dataset for each endmember consisting of attenuated versions of its spectra. The attenuations are multiplicative and range between 0.1 and 1, and so the dataset includes all of the original

(A) Learning features in each material

(a) Spectra in the library pure and scaled

(b) NHMC labels

(c) Probability of high states

(d) Thresholding

(e) Grouping

(g) Features

NHMC parameters: A and σ, obtained in the 1st step

AND

(c) Probability of high states

(d) Thresholding

Other classes

+
−
OR

(f) Feature Rejection

(B) Rejection and detecting each material

(a) Observed Spectra

(b) Mapping to a feature space

NHMC labels

3

6

13

(c) Clustering

Mineral present

Mineral not present

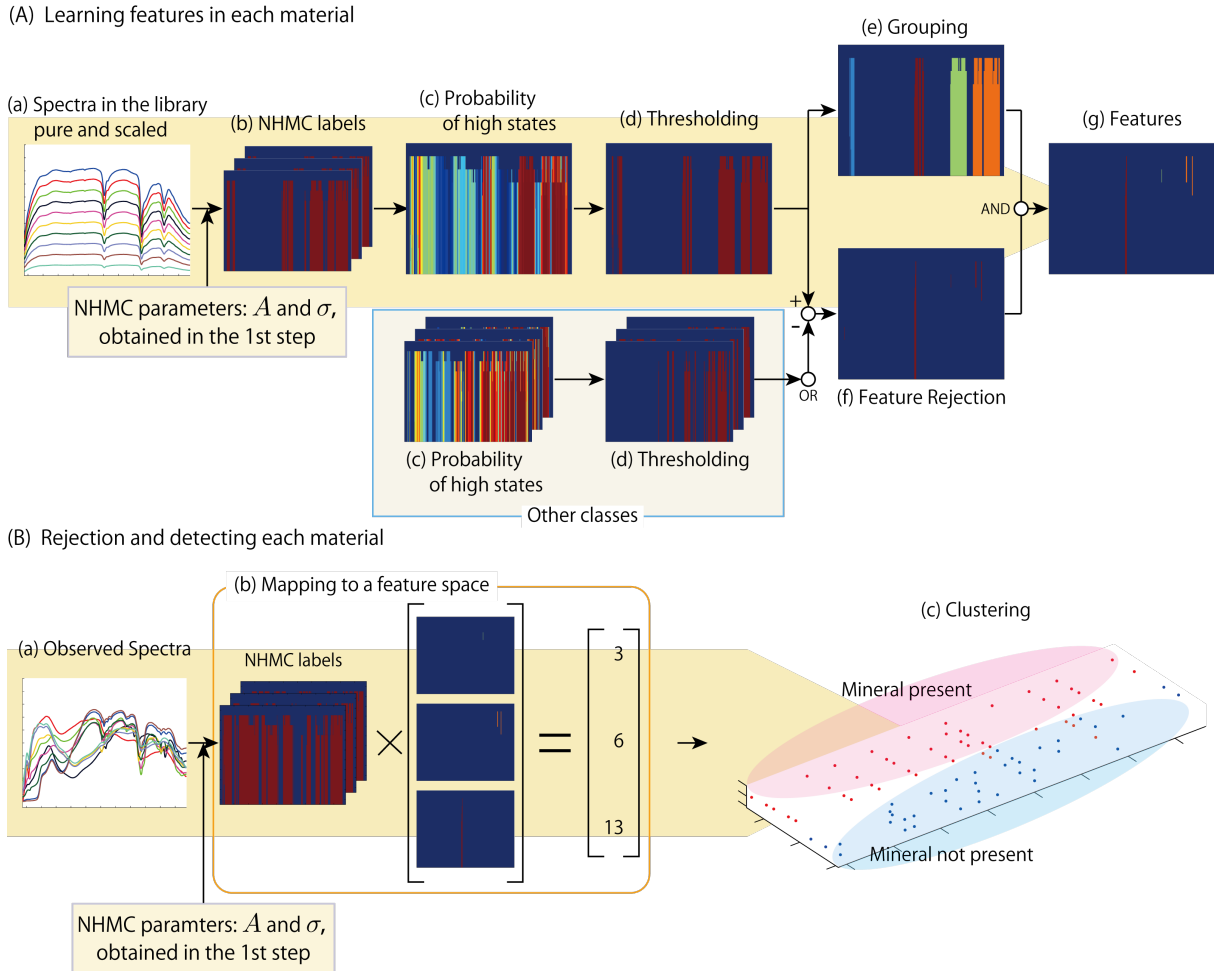NHMC paramters: A and σ, obtained in the 1st step

Fig. 1. Schematic of our algorithm. (A) illustrates the stage where learning features and (B) describes how to detect materials from observations.

endmember spectra (cf. Fig. 1(A)(a)). We then use the NHMC model to obtain binary labels $\mathbf{H}_i^j$ for each one of the spectra $i = 1, 2, \ldots$ in the attenuated dataset for the jth endmember (cf. Fig. 1(A)(b)). The obtained labels are then aggregated through averaging, which effectively provides the percentage of samples among the attenuated spectra for which each label is marked as "large", i.e., $\mathbf{P}^j = \frac{1}{M} \sum_{i=1}^{M} \mathbf{H}_i^j$, where M is the number of samples in the attenuated endmember dataset. After that, we normalize each matrix $\mathbf{P}^j$ by dividing its entries by the value of the largest entry in the matrix. Thus, we can treat $\mathbf{P}^j$ as a normalized probability matrix that provides the likelihood of the "large" state for each wavelet coefficient among the jth endmember dataset (cf. Fig. 1(A)(c)).

In order to focus on the prevalent discriminant features in the endmember spectra, we consider only the labels for those band and scale combinations whose probability of a "large" state in $\mathbf{P}^j$ are larger than the specified threshold value τ, which are then considered as the diagnostic features for the endmember binary labels (cf. Fig. 1(A)(d)). All other labels with probability of "large" state lower than the threshold are eliminated, i.e., we obtain the feature matrix $\hat{\mathbf{P}}^j = I(\mathbf{P}^j > \tau)$, where $I(\cdot)$ is an indicator function. In words, $\hat{\mathbf{P}}^j \in \{0, 1\}^{S \times N}$ is a binary matrix that encodes the set of diagnostic features in the NHMC binary labels for an endmember.

After this thresholding, the selected labels in $\hat{\mathbf{P}}^j$ are

grouped into column clusters. Since spectral absorption features span at least several channels (wavelengths), we assume that labels close enough to each other represent a single spectral feature and we concatenate them together. Similarly, selected labels with less width than the narrowest absorption feature observed in the database should be considered spurious and be removed.

The grouping is performed by first constructing a vector of length equal to the number of wavelengths. The i-th element of such vector is one if the i-th column of the matrix $\hat{\mathbf{P}}^j$ has at least one "large" label, zero otherwise. Afterward, agglomerative hierarchical clustering with single linkage [11] is applied to this vector. The clusters are obtained by cutting the tree so that the maximum distance in any cluster is smaller than a threshold ρ_d. Additionally, clusters exhibiting widths smaller than a threshold ρ_w are discarded. Fig. 1(A)(e) shows the groups (clusters) of features resulting from this stage with different colors.

Independently, we remove features likely to be present in any other material class, which would cause false alarms. To this end, we set another threshold value τ_R that represents the maximum allowance of the high probability state for each selected label in all other classes. If the probability of a "large" state is larger than τ_R for a given band and scale combination in any other class, the corresponding label is eliminated from

the feature under consideration. The outcome of this false-alarm pruning step is a smaller set of features, as illustrated in Fig. 1(A)(f).

Finally, the features that survive the previous step are segmented according to the labels assigned in the grouping step, resulting in F_j discriminative features of one material $\{\mathbf{F}_1^j, \ldots, \mathbf{F}_{F_j}^j\}$ (cf. Fig. 1(A)(g)), where F_j represents the number of clusters and $\mathbf{F}_i^j$ refers to a binary vector indicating the ith cluster obtained from $\hat{\mathbf{P}}^j$.

C. Detection of Endmembers

The NHMC labels for a mixture spectra are assumed to have high similarity to the material's features we introduce because the features learned from each pure and scaled spectra are diagnostic and preserved across many levels of concentration of the material. Based on similarity scores between these binary arrays, we can determine the existence of each material in the observed mixture sample.

To begin, we apply the NHMC model to the observed spectra and obtain their binary label matrix representations $\{\mathbf{X}_n | n = 1, \ldots, N\}$. Next, for each material, similarity scores between the observed spectra and that material's features are computed by taking the matrix inner product between them (cf. Fig. 1(B)(b)): $\sigma_i^j(\mathbf{X}_n) = \left\langle \mathbf{F}_i^j, \mathbf{X}_n \right\rangle$. We collect the similarity scores for a label matrix $\mathbf{X}_n$ with the jth endmember as a vector $\mathbf{y}_n = [\sigma_1^j(\mathbf{X}_n) \ \ldots \ \sigma_{F_j}^j(\mathbf{X}_n)]$.

The process described in this section may be considered altogether as a mapping of the observed spectra into J feature spaces, each of dimension F_j, that measure similarity with the J given endmembers. In these mapped spaces, we apply k-means clustering with $k = 2$ clusters in order to separate observed mixtures involving the endmember from those that do not. After the two clusters are obtained, the cluster whose centroid has larger norm has its samples labeled as "material present", while the samples of the other cluster are labeled "material absent".

III. Experiments

To evaluate the performance of our algorithm, we generate several synthetic spectral mixtures according to a simple version of the Hapke model called the isotropic multiple scattering approximation (IMSA) [6] and we attempt at detecting the endmember using a library of pure mineral spectra. We compare the performance of our algorithm with that of the SUnSAL algorithm [12] applied to the same dataset. We have identified SunSAL as a direct competitor due to its use of a dictionary of spectra for unmixing and to the fact that, although it uses a linear mixing model, it is robust to small nonlinearities [3]. Data clouds generated by the IMSA model have been shown to exhibit only very moderate nonlinearities [13].

A. Performance Metrics

To evaluate the performance of the unmixing algorithms, we use two different measures: *recall* and *false alarm rate* (FAR), defined as $R = \frac{TP}{TP+FN}$, $FA = \frac{FP}{FP+TN}$ where TP and FP are the number of true and false positives, respectively, and TN and FN are the number of true and false negatives, respectively. These metrics are computed for the detectors of materials present in the scene and their average is used as a performance metric for the different unmixing schemes in our experiments.

B. Nonlinear Mixtures with Hapke Model

Our experiment considers a synthetic dataset created by Hapke mixtures model [6]. We extracted 599 spectral signatures with 24 classes in total from the RELAB spectral database[1]. We model our experiments under the assumption that we have some discrepancy between endmembers in the observations and in the library; usually, it is seldom the case to observe the same instance of a spectrum for a material in the endmember library and in the scene. Under such assumption, we divide the available data into two sets (endmember and scene) so that elements in the endmember library and the observations for each mineral class are maximally different. For this purpose, we apply k-means clustering with $k = 2$ using cosine distance to each mineral class to maximize the discrepancy. The resulting endmember set used for training has 357 samples, while the test set used for constructing mixtures has 242 samples.

Once the test set is obtained, we construct three different subsets from it containing three endmembers each, and generate 2000 mixtures from each subset according to IMSA model; we thus obtain 6000 synthetic IMSA mixtures without any noise. To mimic the variability of endmembers in the same mineral class, we constructed different endmembers by IMSA mixtures of the samples in the same mineral classes instead of selecting the endmembers from the library directly. The abundances in each mixture are generated according to a symmetric Dirichlet distribution of order $K = 3$ with concentration parameter $\alpha = 1$. All the RELAB spectra in this experiment were acquired incident i and emission e angles of $30°$ and $0°$ respectively. We set the same values for i and e of the IMSA mixtures.

We apply the proposed NHMC-based endmember detection method and the SUnSAL algorithm to each synthetic mixture. We assume the exact mineral classes are obtained by an oracle dictionary pruning method before applying either unmixing method.

In a first experiment, we investigate the performance of our proposed method and SUnSAL and search for the best parameter values over fixed ranges. For our method, τ and τ_R are searched in $[0.1 : 0.1 : 1.0]$. Additionally, we set $\rho_d = 4$ and $\rho_w = 5$. The SUnSAL trade-off parameter λ, which controls the sparsity of the result, is searched in the exponential range $10^{[-5:1:2]}$. Figures 2 and 3 show the performance for the two unmixing approaches. Figure 2 demonstrates the performance curve of SUnSAL as λ varies. Broadly, it can be seen that R decreases and FA increases as λ increases, and vice versa. When we define the optimal point as the closest point to the upper left corner of the figure, the optimal value obtained by SUnSAL is $R = 0.80$ and $FA = 0.23$, at $\lambda = 0.1$. Similarly, Figure 3 presents the performance curves of the proposed method for different values of τ_R, with τ fixed for each curve. The defined optimal point obtained by our method is $R = 0.83$ and $FA = 0.20$ at $\tau = 0.7$ and $\tau_R = 0.7$, which shows a slight improvement over that obtained from SUnSAL.

An important observation is that the proposed binary representation is robust with respect to the spectral variability present in each mineral class. We calculate the separation between the training and test subset clusters for all the mineral classes in the original space and in the space of the NHMC
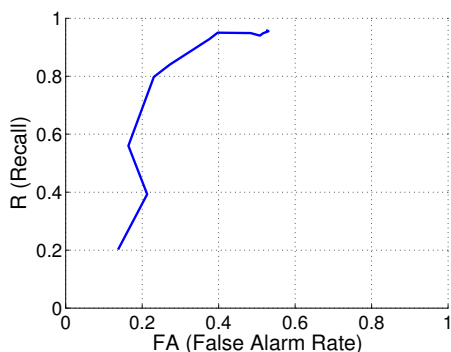

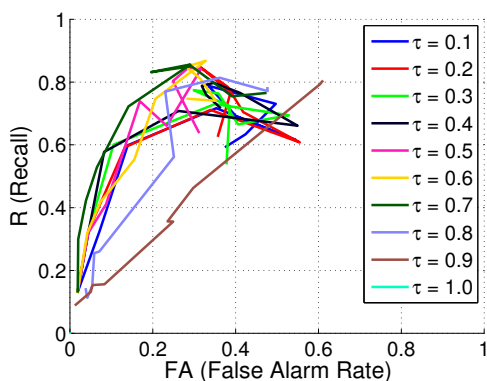Fig. 2. Performance curve of the SUnSAL

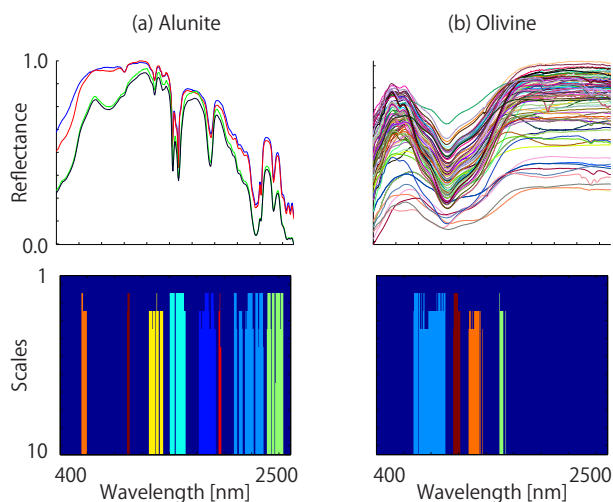Fig. 3. Performance curve of our method: each curve is drawn with τ fixed.

Fig. 4. Top: Spectra of Alunite and Olivine in the endmember library; bottom: their diagnostic features detected by the NHMC model.

labels. The separation was defined as the ration of the sum of the within cluster distances and the sum of the between cluster distances. We observed that well separated training and test clusters in the original space are mostly overlapping in feature space (for example for kaolinite the separability measure was 11.01 in the original space and 0.7 in feature space, for actinolite 21.51 and 2.89).

IV. DISCUSSION ABOUT SPECTRAL FEATURES

Our method returns diagnostic features of each endmember as byproducts, which make it easy for practitioners to interpret

the physical characteristics of each material. Fig. 4 shows diagnostic features of alunite and olivine detected by our method that persist through the mixing process. Our method seems to succinctly detect discontinuities and slopes of each mineral. More specifically, it detects the same diagnostic features of alunite around $2.2 - 2.4\mu m$ regions as the ones defined by geologists in the Tetracorder.

V. CONCLUSION

We demonstrate a new spectral unmixing method using a new semantic representation. The simulation in which we mimic the real condition shows that our method yields slightly better detection performance compared to a state-of-the-art method. This fact indicates that the underlying model has a possibility to successfully determine discriminative features of the spectra and we could use them for unmixing problems. Further investigation is needed to improve the performance.

REFERENCES

[1] J. M. B. Dias, A. Plaza, N. Dobigeon, M. Parente, Q. Du, P. Gader, and J. Chanussot, "Hyperspectral unmixing overview: geometrical, statistical, and sparse regression-based approaches," *J. Selected Topics in Applied Earth Observations and Remote Sensing*, vol. 5, no. 2, pp. 354–379, 2012.

[2] N. Dobigeon, J.-Y. Tourneret, C. Richard, J. Bermudez, S. McLaughlin, and A. Hero, "Nonlinear unmixing of hyperspectral images: Models and algorithms," *Signal Processing Magazine, IEEE*, vol. 31, no. 1, pp. 82–94, Jan 2014.

[3] M.-D. Iordache, J. Bioucas-Dias, and A. Plaza, "Sparse unmixing of hyperspectral data," *IEEE Trans. Geoscience and Remote Sensing*, vol. 49, no. 6, pp. 2014–2039, June 2011.

[4] M.-D. Iordache, J. Bioucas-Dias, A. Plaza, and B. Somers, "Music-csr: Hyperspectral unmixing via multiple signal classification and collaborative sparse regression," *IEEE Trans. Geoscience and Remote Sensing*, vol. 52, no. 7, pp. 4364–4382, July 2014.

[5] M.-D. Iordache, J. Bioucas-Dias, and A. Plaza, "Collaborative sparse regression for hyperspectral unmixing," *IEEE Trans. Geoscience and Remote Sensing*, vol. 52, no. 1, pp. 341–354, Jan. 2014.

[6] B. Hapke, *Theory of reflectance and emittance spectroscopy*. Cambridge University Press, 2012.

[7] R. N. Clark, G. A. Swayze, K. E. Livo, R. F. Kokaly, S. J. Sutley, J. B. Dalton, R. R. McDougal, and C. A. Gent, "Imaging spectroscopy: Earth and planetary remote sensing with the USGS Tetracorder and expert systems," *J. Geophys. Res.*, vol. 108, no. E12, 5131, pp. 5–1 to 5–44, December 2003, doi:10.1029/2002JE001847. [Online]. Available: http://speclab.cr.usgs.gov/PAPERS/tetracorder

[8] M. Parente and M. F. Duarte, "A new semantic wavelet-based spectral representation," in *IEEE Workshop on Hyperspectral Image and Signal Processing: Evolution in Remote Sensing (WHISPERS)*, Gainesville, FL, June 2013.

[9] M. F. Duarte and M. Parente, "Non-Homogeneous Hidden Markov Chain Models for Wavelet-Based Hyperspectral Image Processing," in *Allerton Conf. Communication, Control, and Computing*, IL, Oct. 2013.

[10] S. Feng, Y. Itoh, M. Parente, and M. F. Duarte, "Tailoring non-homogeneous markov chain wavelet models for hyperspectral signature classification," in *IEEE Int. Conf. Image Processing (ICIP)*, Paris, France, Oct. 2014.

[11] T. Hastie, R. Tibshirani, and J. Friedman, *The Elements of Statistical Learning*, 2nd ed. New York, NY: Springer, 2009.

[12] J. M. Bioucas-Dias and M. A. T. Figueiredo, "Alternating direction algorithms for constrained sparse regression: Application to hyperspectral unmixing," in *IEEE Workshop on Hyperspectral Image and Signal Processing: Evolution in Remote Sensing (WHISPERS)*, Reykjavik, Iceland, June 2010.

[13] A. M. Saranathan and M. Parente, "Unmixing multiple intimate mixtures using manifold clustering," in *IEEE Workshop on Hyperspectral Image and Signal Processing: Evolution in Remote Sensing (WHISPERS)*, Lausanne, Switzerland, June 2014.